Acta Polytechnica **60**(3):268–278, 2020
DOI:10.14311/AP.2020.60.0268

available online at https://ojs.cvut.cz/ojs/index.php/ap

ON THE SECOND LIGHT FLASH EMITTED FROM A SPARK-GENERATED BUBBLE OSCILLATING IN WATER

Karel Vokurka

Technical University of Liberec, Physics Department, Studentská 2, 461 17 Liberec, Czech Republic
correspondence: karel.vokurka@tul.cz

Abstract. The light emitted from the spark-generated bubbles oscillating in water is studied experimentally. Attention is paid to the emission of light from bubbles in the final stages of their first contraction and in the early stages of their following expansion. In some experiments, two close flashes of light were observed. The first light flash has already been studied in earlier works. In the present work, attention is paid to the second light flash. The relations between the first and second flashes of light and the size of the bubbles are studied and discussed in detail. It is assumed that these two light flashes are caused by two different processes taking place in the bubbles. The possible nature of these two processes is briefly discussed.

Keywords: Spark-generated bubbles, bubble oscillations, light emission.

1. Introduction

The physical processes taking place in bubbles oscillating in liquids are very complex. Although much effort has been devoted to clarifying these physical processes, many issues in this field are still not well understood. For example, a great deal of works has been devoted to clarifying the processes responsible for cavitation erosion (see, e.g., reference [1]). However, the specific mechanism responsible for cavitation erosion has not yet been satisfactorily identified. The emission of light from oscillating bubbles, which will be studied in this work, represents another unexplained problem. Other studies of bubble oscillations have focused on improving contrast-enhancement in medical ultrasonic imaging [2–6], and even in this case, a better understanding of the physical processes running in bubbles may be useful.

Oscillating bubbles are generated in laboratory experiments by many techniques, such as by focussing a laser beam into liquid [7–13], spark discharge in liquid [14–19], irradiating liquid with intense ultrasonic waves (acoustic cavitation) [20], or in a liquid flow (hydrodynamic cavitation) [21]. All these techniques are also used in studies of light emission from bubbles [8–13, 15–18, 20, 21].

Over the last three decades, the emission of light from a single bubble oscillating in acoustic resonators has also been intensively studied (see, e.g., a recent review [22], which summarises results from 163 works). An advantage of a method based on acoustic resonators is that relatively small experimental set-ups can be used. However, a serious disadvantage of this technique is that only small bubbles are generated which have maximum radii of less than 100 µm. These small bubbles oscillate very quickly, and therefore all the physical processes that take place in them also run very fast, which makes their study difficult. Measuring light flashes from these small sources at relatively large distances requires averaging, during which many important features are lost. And measuring ultrasonic waves radiated by these bubbles is also a difficult task because spectral components of these waves are ranging up to several hundreds of MHz.

In the present work, the emission of light from large spark-generated bubbles freely oscillating in water far from boundaries is studied. As mentioned in earlier works [23–25], the large spark-generated bubbles have many advantages that will also be exploited in this study. During the study of the light flashes radiated from these bubbles in the final stages of their first contraction and early stages of the following expansion, we occasionally observed that the first flash of light was accompanied by a slightly delayed second flash of light. Whereas the first flashes have been studied in detail in [24, 25], in this work we want to concentrate on the second flashes. In Section 3, the time distance between the two flashes, the maximum values of these flashes, and the position of the two flashes relative to the position of the pressure pulse (and thus also with respect to an instant when the bubble is contracted to its first minimum volume) will be studied in detail. Multiple secondary light flashes have also been observed by Ohl [9], Sukovich et al. [12], Supponen et al. [13] and Moran and Sweider [26]. However, in these works, secondary light pulses have not been studied in detail and no concurrently emitted pressure pulses have been used to analyse the observed events in the time domain.

2. Experimental setup and nomenclature

The data analysed and discussed in this work are a subset of the data already presented in the works [24, 25]. This means that the data were obtained using the same experimental setup. Therefore, only a brief de-

scription of the instruments, the measuring procedure, and the nomenclature will be given here. Further details can be found in [24, 25].

The freely oscillating bubbles were generated by spark discharges in a large laboratory water tank having dimensions 4 m (width), 6 m (length), and 5.5 m (depth). The sparker used in the experiments consisted of two thin tungsten electrodes having a diameter of 1 mm and a length of 50 mm. The electrode tips were facing each other and were separated by a narrow gap. Due to electrode burning the length of the gap in subsequent experiments gradually increased from about 0.2 mm to 3 mm. The tungsten electrodes were mounted in conical brass holders and were connected by cables to a condenser bank, whose capacitance could be varied in 10 steps from 16 uF to 160 uF. The capacitors were charged from a high voltage source of 4 kV, and an air-gap switch was used to trigger the discharge. After closing the air-gap switch, at a time t_0 the liquid breakdown occurs and the discharge channel starts growing explosively. This explosive growth is accompanied by intensive light (optical) emission and pressure (acoustic) wave radiation from the bubble.

The explosively growing almost spherical bubble attains its first maximum volume at time t_1 and has a radius R_{m1}. Then the bubble starts contracting. At time t_{c1}, the bubble contracts to its first minimum volume. Although very little is currently known about the shape of the contracted bubble, it will be assumed that it is a sphere having radius R_{M1}. Then the bubble starts expanding and at time t_2 attains its second maximum volume and has a radius R_{M2}. Further bubble oscillations follow, but these are beyond the scope of this work. In the following, the interval (t_0, t_1) will be referred to as the initial growth phase, the interval (t_1, t_{c1}) as the first contraction phase, and the interval (t_{c1}, t_2) as the first expansion phase of the bubble.

Prior to the measurements reported here, a limited number of high-speed camera films were taken with framing rates ranging from 2800 to 3000 frames/s. These records were used to check the shape of the generated bubbles. Besides, the photographs yielded useful visual information about the bubble content. Examples of images of spark-generated bubbles can be seen in earlier works [23, 27].

Both the spark discharge and the subsequent bubble oscillations are accompanied by an intensive emission of light and pressure waves. A relatively simple arrangement was used to record the optical waves. A fibre optic cable was fixed at the same depth in water as the sparker. The input surface of this cable was pointing perpendicularly to the electrodes and was positioned at a distance $r = 0.2$ m from the sparker gap. A photodiode was positioned at the other end of the fibre optic cable. The output voltage $u(t)$ from the photodiode was amplified, digitized and stored in a computer. The record of the optical radiation $u(t)$ can be divided into two pulses. First, it is the pulse $u_0(t)$ that was emitted during the interval (t_0, t_1), and second, it is the pulse $u_1(t)$ that was emitted during the interval (t_1, t_2). In this work, only the pulses $u_1(t)$ will be considered and the instant, at which the pulse $u_1(t)$ attains the maximum value u_{M1} will be denoted as t_{u1}.

The pressure waves $p(t)$ were recorded using a broadband hydrophone, which was positioned at the same depth as the sparker at a distance $r_h = 0.2$ m from the gap of the sparker. The hydrophone output voltage was digitized and stored in a computer. Like the optical wave, the pressure wave $p(t)$ can be divided into two pulses. First, it is the pressure pulse $p_0(t)$ that was radiated during the interval (t_0, t_1), and second, it is the pressure pulse $p_1(t)$ that was radiated during the interval (t_1, t_2). Only the pulse $p_1(t)$ will be considered in this work. The instant, at which the pressure pulse $p_1(t)$ attains the peak value p_{p1} , will be denoted as t_{p1}.

The sparker was submerged in water at a depth of $h = 2.5$ m (ie. at hydrostatic pressure p_∞) far away from the tank walls. Generated bubbles can be described by two parameters. First, it is the bubble size R_{M1}, and second, it is the bubble oscillation intensity p_{zp1} (this parameter is defined as $p_{zp1} = (p_{p1} \cdot r_h)/(p_\infty \cdot R_{M1})$). Both R_{M1} and p_{zp1} were determined in each experiment from the respective pressure record using an iterative procedure described in [23]. The sizes R_{M1} of the bubbles studied in this work ranged from 21 mm to 56.5 mm, the bubble oscillation intensities p_{zp1} ranged from 92.4 to 152.8.

The pressure wave propagates from the bubble wall to the hydrophone at the speed of sound in water. Therefore, the times t_0, t_1 and t_2 in the pressure record are delayed by about 135 µs after the times t_0, t_1, and t_2 in the optical record. However, as shown in [25], the instants of the liquid breakdown t_0 can be determined in both records $u(t)$ and $p(t)$ with a precision 0.1 µs. The pressure record can thus be shifted along the time axis so that the times t_0 in both records are identical. Examples of the whole records $u(t)$ and $p(t)$ were presented in [25]. In this work, only small portions of the pulses $u_1(t)$ and $p_1(t)$ extracted from the records in the vicinity of t_{u1} and t_{p1} will be displayed and discussed in the following text. And even if it has not been verified experimentally yet, in the following discussion, it will be assumed that the peak pressure in the pulse $p_1(t)$ is radiated at the same instant the bubble is contracted to the first minimum volume. In other words, in the following discussion it is assumed that in the shifted pressure record $t_{p1} = t_{c1}$.

In earlier studies of light emission in the interval (t_1, t_2) from the spark-generated bubbles, a total of 98 experiments were quantitatively evaluated [24, 25]. In a prevailing part of these experiments, a single light flash was observed. An example of a typical single pulse $u_1(t)$ is shown in Figure 1. In [24] the single optical pulses were analysed and characterized

by three parameters: the maximum voltage u_{M1} in the pulse, the time t_{u1} of occurrence of maximum voltage, and the pulse width Δ at the half value of the maximum voltage (that is the pulse width at $u_{M1}/2$). All these parameters are displayed in Figure 1. In [25], it was further shown that the light flashes $u_1(t)$ are not radiated from the bubble synchronously with the pressure pulses $p_1(t)$, but the light flashes are radiated either a bit earlier or a bit later than the pressure pulses. The difference between times t_{u1} and t_{p1} was denoted as δ_1 and was defined as $\delta_1 = t_{u1} - t_{p1}$.

In some experiments (exactly in 22 of 98 experiments), beside the first optical pulse $u_1(t)$, a second optical pulse $u_2(t)$, slightly delayed after the first pulse, was also observed. An example of a record, where both the first pulse $u_1(t)$ and the second pulse $u_2(t)$ can be seen, is given in Figure 2. The situation, when two pulses are present in the record, can be characterized by six parameters: the maximum voltages u_{M1} and u_{M2} in pulses, the times of occurrence of these maxima t_{u1} and t_{u2}, the distance d_{12} between the times t_{u1} and t_{u2} (this parameter is defined as $d_{12} = t_{u2} - t_{u1}$), and the pulse width Δ introduced already earlier for a single pulse $u_1(t)$. It is evident that now pulse width Δ describes two pulses, which are more or less melted together. However, there is currently no way to separate the two pulses from each other. In defining the mutual position of the second light pulse $u_2(t)$ and the pressure pulse $p_1(t)$ on the time axis we will proceed in the same way as in the case of the time difference δ_1. The difference between times t_{u2} and t_{p1} will be denoted as δ_2 and is defined as $\delta_2 = t_{u2} - t_{p1}$. The parameters describing the position of the two optical pulses $u_1(t)$ and $u_2(t)$ and the acoustic pulse $p_1(t)$ on the time axis are shown in Figure 3.

3. RESULTS

In the experiments analysed here, pulses $p_1(t)$, $u_1(t)$ and $u_2(t)$ were radiated from almost spherical bubbles [24, 25]. The sizes of these bubbles are described by the first maximum radius R_{M1} and the bubble oscillation intensities are described by the non-dimensional peak pressure in the first acoustic pulse p_{zp1}. Thus, there are eight parameters available that can be used in the analysis: six parameters describing pulses $u_1(t)$ and $u_2(t)$ and their time position with respect to pulse $p_1(t)$ and two parameters describing the bubble itself. Using the data from 22 experiments, where second light pulses were observed, a correlation analysis was done between these eight parameters, that is between d_{12}, δ_1, δ_2, u_{M1}, u_{M2}, Δ, R_{M1}, and p_{zp1}. In most of these analyses, it was noticed that the correlation between selected parameters is very weak. Such weak correlation can be seen, for example, in cases where the bubble oscillation intensity p_{zp1} was entered as one of the two parameters into the analysis. This weak correlation of optical radiation with the intensity of bubble oscillation was already observed in references [24, 25] and was used as a proof for the assertion concerning the relative autonomous behaviour of plasma in the bubble interior. Some other weak correlations have also been observed. As these weak correlations currently do not provide any new information, they will not be considered any further and only the dependences of the selected parameters will henceforth be discussed. These are variations of d_{12}, δ_2, u_{M2}, and u_{M2}/u_{M1} with R_{M1}, d_{12} with Δ, and δ_1 with d_{12}. These variations are shown in Figures 4 - 9.

In Figure 4, the variation of the time distance d_{12} between the two optical pulses $u_2(t)$ and $u_1(t)$ with the bubble size R_{M1} is shown. The regression line for the mean value of d_{12} in dependence on R_{M1} is $< d_{12} >= 0.27R_{M1} - 4.55$ [µs, mm]. It can be seen that d_{12} is only very weakly correlated with R_{M1} and that the dispersion of d_{12} increases with R_{M1}. The variation of d_{12} with R_{M1} agrees with the correlation between d_{12} and Δ shown later in Figure 8 (d_{12} grows with Δ) and with the correlation between Δ and R_{M1} shown in Figure 9 in [24] (Δ grows with the bubble size as $\sim R_{M1}^{3.3}$). However, now the quantities d_{12} and R_{M1} are only weakly correlated. This is in contrast to the moderate correlation of d_{12} with Δ shown in Figure 8, and Δ with R_{M1}, shown in Figure 9 in [24].

In Figure 5, the variation of the time difference δ_2 between the radiation of the second light pulse $u_2(t)$ and the pressure pulse $p_1(t)$ with the bubble size R_{M1} is shown. The regression line for the mean value of δ_2 in dependence on R_{M1} is $< \delta_2 >= 0.097R_{M1} - 1.12$ [µs, mm]. It can be seen that δ_2 is correlated with R_{M1} only weakly and that the dispersion of δ_2 increases with R_{M1}. The time difference δ_2 grows with the bubble size R_{M1}. This is also in an agreement with the variation of distance d_{12} with the pulse width Δ given in Figure 8 (distance d_{12} is part of Δ and equals $d_{12} = \delta_2 - \delta_1$). And it is also in an agreement with previous results concerning the variation of the pulse width Δ with R_{M1} (Figure 9 in [24]). It can be seen in Figure 5 that δ_2 was positive in all experiments reported here, which means that the second light flashes were always (with the exception of a single experiment, in which $\delta_2 = 0$) radiated some µs after the time t_{c1} when the bubbles were contracted to minimum volumes. However, as can be seen in Figure 7 in [25], the time difference δ_1 between the radiation of the first optical pulse $u_1(t)$ and the pressure pulse $p_1(t)$ was negative in the prevailing number of experiments. This means that the first light flashes $u_1(t)$ are usually radiated a few µs before the bubbles have been contracted to minimum volumes at t_{c1}, which is in contrast to the second light flashes $u_2(t)$ that were radiated some µs after the bubbles have been contracted to minimum volumes.

In Figure 6, the variation of the maximum voltage u_{M2} in the optical pulse $u_2(t)$ with the bubble size R_{M1} is shown. The regression quadratic polynomial for the mean value of u_{M2} in dependence on R_{M1} is

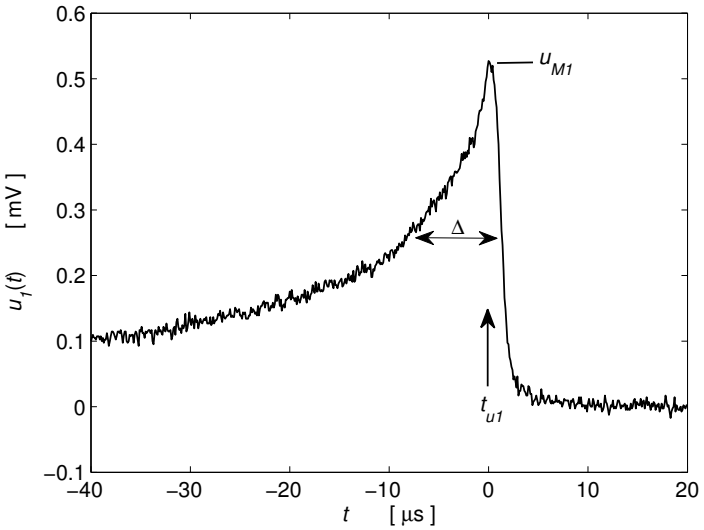

FIGURE 1. Detailed view of pulse $u_1(t)$ at the output of the optical detector. The spark-generated bubble has a size of $R_{M1} = 49\,\text{mm}$, and oscillates with an intensity of $p_{zp1} = 142.1$. In this figure, the time axis origin is set at t_{u1} and from the pulse $u_1(t)$, only a small portion near t_{u1} is shown. The width of this pulse is $\Delta = 9.4\,\mu\text{s}$ and the difference between times t_{u1} and t_{p1} is $\delta_1 = -2.6\,\mu\text{s}$.

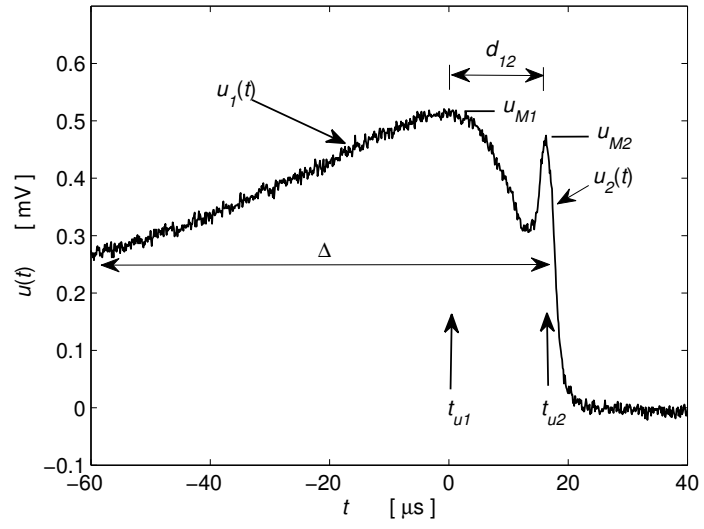

FIGURE 2. Detailed view of pulses $u_1(t)$ and $u_2(t)$ at the output of the optical detector. The spark-generated bubble has a size of $R_{M1} = 53.6\,\text{mm}$, and oscillates with an intensity of $p_{zp1} = 98.0$. In this figure, the time axis origin is set at t_{u1} and from the two pulses, only a small portion near t_{u1} is shown. The width of the two partially merged pulses is $\Delta = 83.6\,\mu\text{s}$ and the difference between times t_{u1} and t_{p1} is $\delta_1 = -11\,\mu\text{s}$.

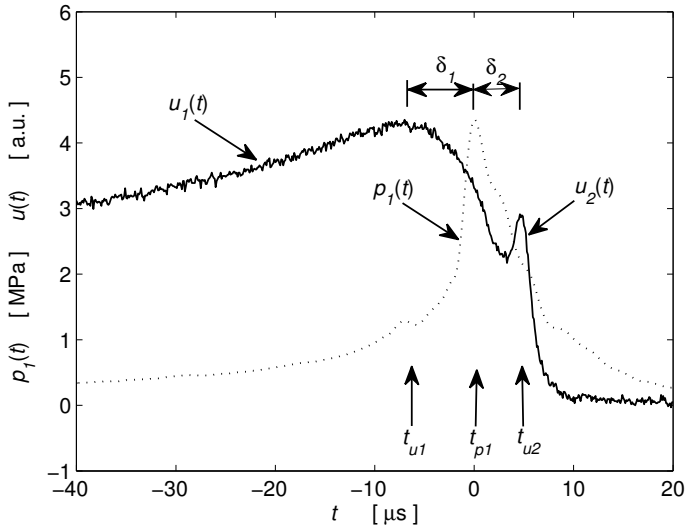

FIGURE 3. Example of optical and pressure waves in the vicinity of the times t_{u1} and t_{p1} (to display both waves in comparable sizes, the wave $u(t)$ is shown in [a.u.]).The bubble size is $R_{M1} = 56.5\,\mathrm{mm}$, the intensity of bubble oscillation is $p_{zp1} = 127.3$. Time differences in the occurrence of maxima in both optical pulses with respect to the pressure pulse are $\delta_1 = -7.0\,\mu\mathrm{s}$ and $\delta_2 = 4.6\,\mu\mathrm{s}$. In this figure, the time axis origin is set at t_{p1} and only small portions near t_{u1}, t_{p1} and t_{u2} are shown from the optical record $u(t)$ and acoustic record $p(t)$.

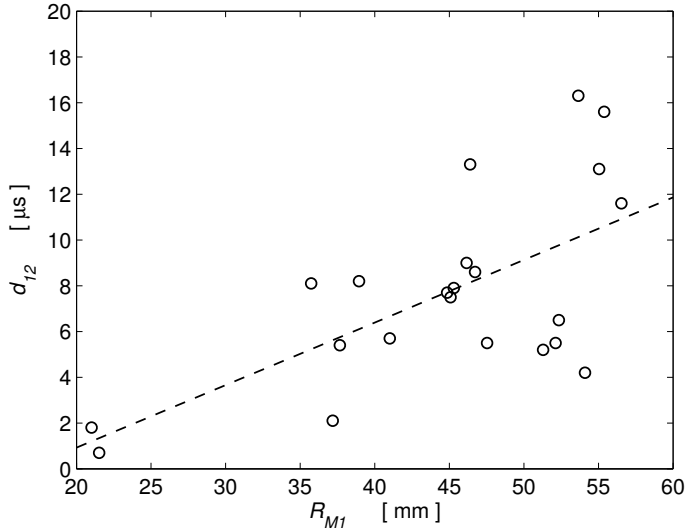

FIGURE 4. Variation of the time distance between the first and second optical pulses d_{12} with bubble size R_{M1}.

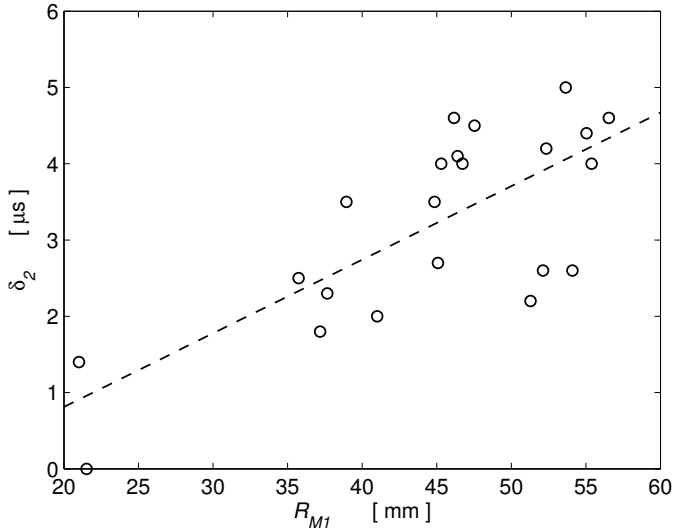

FIGURE 5. Variation of the time difference between the occurrence of the second optical pulse and the acoustic pulse δ_2 with bubble size R_{M1}.

$< u_{M2} >= 2.3 \times 10^{-4} R_{M1}^2 - 6.2 \times 10^{-3} R_{M1} + 3.9 \times 10^{-2}$ [mV, mm]. It can be seen that u_{M2} is weakly correlated with R_{M1} and grows with the bubble size as $\sim R_{M1}^2$.

In Figure 7, the variation of the ratio u_{M2}/u_{M1} with the bubble size R_{M1} is shown. The regression line for the mean value of the ratio u_{M2}/u_{M1} in dependence on R_{M1} is $< u_{M2}/u_{M1} >= -0.004 R_{M1} + 0.87$ [- , mm]. It can be seen that the ratio u_{M2}/u_{M1} is correlated with R_{M1} only very weakly and that, in most of the experiments, $u_{M1} > u_{M2}$. The ratio u_{M2}/u_{M1} is almost independent of the bubble size R_{M1}. This is in an agreement with the fact that u_{M2} grows with R_{M1} as $\sim R_{M1}^2$ (Figure 6) and u_{M1} grows with R_{M1} as $\sim R_{M1}^{2.5}$ [24].

The variation of the time distance d_{12} between optical pulses $u_2(t)$ and $u_1(t)$ with the pulse width Δ is shown in Figure 8. The regression line for the mean value of d_{12} in dependence on Δ is $< d_{12} >= 0.15\Delta + 1.62$ [µs, µs]. It can be seen that d_{12} is moderately correlated with Δ. The moderate correlation between d_{12} and Δ is what could be expected, viz. that the distance d_{12} is larger for broader pulses (larger Δ) and smaller for narrower pulses (smaller Δ).

The variation of the time difference δ_1 between the first light pulse $u_1(t)$ and the pressure pulse $p_1(t)$ with the time distance d_{12} between optical pulses $u_2(t)$ and $u_1(t)$ is shown in Figure 9. The regression line for the mean value of δ_1 in dependence on d_{12} is $< \delta_1 >= -0.79 d_{12} + 1.65$ [µs, µs]. It can be seen that δ_1 is moderately correlated with d_{12}. As can also be observed, the bubbles with larger time distance d_{12} between optical pulses $u_2(t)$ and $u_1(t)$ radiate the first optical pulse more early before the bubble is contracted to the minimum volume at t_{c1}. This finding can be compared with Figure 7 in [25], where the variation of δ_1 with R_{M1} is given and where it is shown that for larger bubbles, δ_1 is larger, too. And as shown in Figure 9 in [24], for larger bubbles, the widths Δ are also larger. Finally, as shown in Figure 8, the distance d_{12} grows with the pulse width Δ, hence it can be expected that δ_1, in absolute values, will grow with d_{12} as well, a fact that is confirmed in Figure 9.

In conclusion, it may be said that the variances of the parameters discussed above are in an agreement with the results set forth in references [24, 25]. Unfortunately, at the current state of knowledge of the processes taking place in oscillating bubbles, no deeper physical explanation of the observed correlations is possible. The processes that may be responsible for the observed phenomena are briefly discussed in the following Section.

4. DISCUSSION

Although the light emission from oscillating bubbles has been intensively studied in many laboratories for several decades (see, e.g., works [8–13, 15–18, 20, 21, 26], and the recent review by Borisenok [22]), only very limited quantitative experimental data are still available at present, and therefore understanding of the physical or chemical processes taking place in oscillating bubbles is currently very difficult. In a review paper [22], many theories trying to explain the light emission from oscillating bubbles are mentioned, but none of the theoretical models can explain the experimental data presented in this work and in references [24, 25, 27, 28]. For example, as can be seen in Figures 2, 3 and 5, the shape of the pulses $u_1(t)$ and $u_2(t)$ and their timing with respect to the bubble wall motion at first sight exclude the "hot spot" theory preferred by most researchers [22]. And both the shape of the pulse $p_1(t)$ (single pulse) and its position relative to the pulses $u_1(t)$ and $u_2(t)$ exclude the explanation

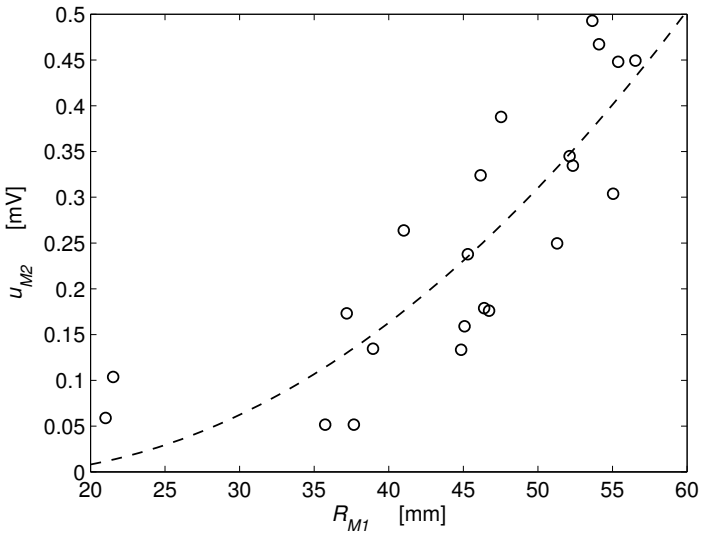

FIGURE 6. Variation of the maximum voltage in the second optical pulse u_{M2} with bubble size R_{M1}.

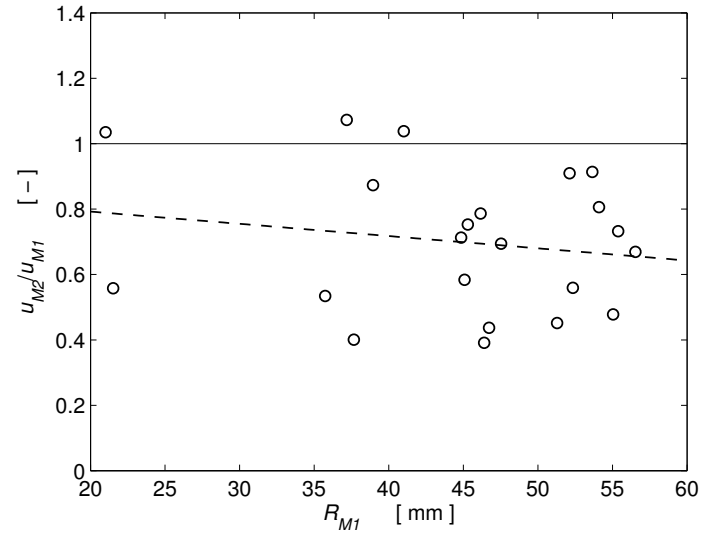

FIGURE 7. Variation of the ratio of maximum voltages in the first and second optical pulses u_{M2}/u_{M1} with bubble size R_{M1}.

of the two light flashes by the bubble splitting in the final stages of the contraction and early stages of the following expansion into two parts. And although the values of the parameters $d_{12}, \delta_1, \delta_2, u_{M1}, u_{M2}$, and Δ may vary in different experiments (see, Figs 4 - 9), the shapes of the pulses $u_1(t)$ and $u_2(t)$ were always similar to the shapes shown in Figs. 2 - 3. And this also contradicts to the possible explanation that the bubble was split into several parts, because such a splitting can be expected to be random.

From the optical records on which both pulses $u_1(t)$ and $u_2(t)$ are simultaneously present, it is evident that there are two physical or chemical processes taking place in a bubble. The first process is responsible for the emission of the optical pulse $u_1(t)$. The second process is responsible for the emission of the optical pulse $u_2(t)$. Based on the experimental data published in references [24, 25, 27, 28], where the long-lasting and very autonomously behaving plasma in bubbles was described, the author of this work came to the conclusion that in the interior of spark-generated bubbles, during their first oscillation, plasmoids are present (and not the usual plasma) and that these plasmoids are responsible for the emission of light pulses $u_1(t)$ [25] (the presence of these plasmoids in the bubble interior is clearly seen, for example, in images presented in Figure 2 in [27]). As mentioned already in [25], similar nonstandard plasma generated by electric discharges in water has been studied, e.g., by Egorov et al. [29]. These authors talk about autonomous glowing plasma (or about plasmoids) and refer to the works of Shevkunov [30, 31], where the process of interaction between H_2O molecules and H^+ and OH^- ions in air containing water vapour is mod-

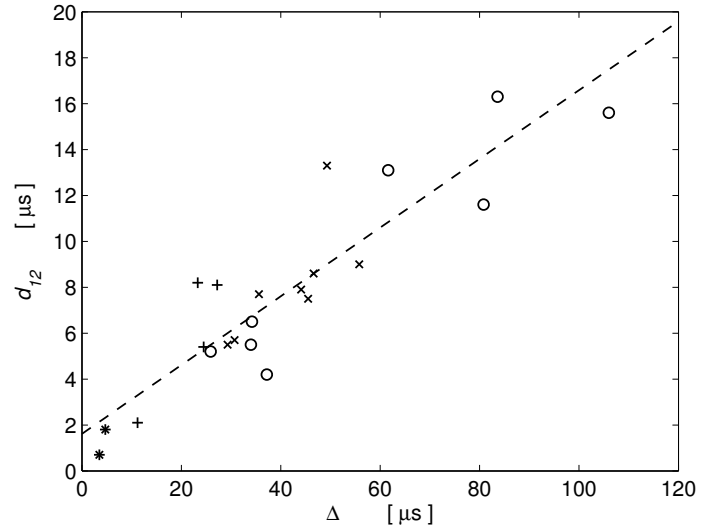

FIGURE 8. Variation of the time distance between the first and second optical pulses d_{12} with optical pulse width Δ. Bubble sizes: 'o' $R_{M1} > 50\,\text{mm}$, 'x' $50\,\text{mm} \geq R_{M1} > 40\,\text{mm}$, '+' $40\,\text{mm} \geq R_{M1} > 30\,\text{mm}$, '*' $30\,\text{mm} \geq R_{M1} > 20\,\text{mm}$, '.' $20\,\text{mm} \geq R_{M1}$.

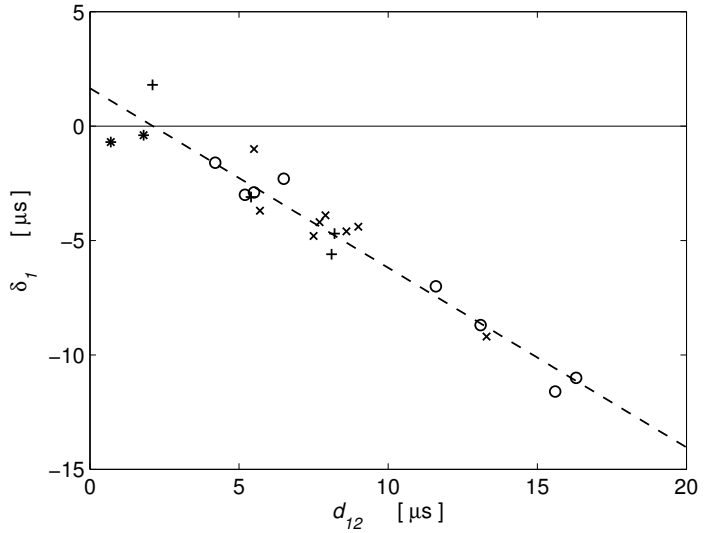

FIGURE 9. Variation of the time difference in the occurrence of the first optical pulse and the pressure pulse δ_1 with time distance between the first and second optical pulse d_{12}. Bubble sizes: 'o' $R_{M1} > 50\,\text{mm}$, 'x' $50\,\text{mm} \geq R_{M1} > 40\,\text{mm}$, '+' $40\,\text{mm} \geq R_{M1} > 30\,\text{mm}$, '*' $30\,\text{mm} \geq R_{M1} > 20\,\text{mm}$, '.' $20\,\text{mm} \geq R_{M1}$.

elled to explain the phenomenon of long-lasting and glowing plasma. Independently of Egorov et al. [29], Golubnichy et al. [15] also studied nonstandard plasma in bubbles generated by electric discharges in water and in this case, the authors call this form of plasma as "long-living luminous objects" (LLLO).

It may also be interesting to note that, while the pulse $u_1(t)$ was observed independently on the bubble oscillation intensity p_{zp1} in all experiments, the pulse $u_2(t)$ was only observed when studying bubbles oscillating with an intensity of $p_{zp1} > 92$. However, as mentioned in Section 3, only very weak correlation of the studied parameters $d_{12}, \delta_1, \delta_2, u_{M1}, u_{M2}$, and Δ with intensity of bubble oscillations p_{zp1} was observed, and therefore no scatter plots of these parameters were presented.

In the present paper, the shapes of the second light pulses $u_2(t)$ and their position on the time axis relative to the position of the pressure pulses (and thus implicitly also relative to the instantaneous motion of the bubble wall) were studied in a greater detail. From Figures 2, 3, and 7, it is evident that to explain the existence of the second light pulses, a new physical or chemical process taking place in spark-generated bubbles must be considered. It is highly probable that the process responsible for the emission of the light pulses $u_2(t)$ is always present in the bubble, but the light emitted by this process is very often overlapped by the light emitted from the contracted (and thus heated) plasmoid. Therefore, only a single flash of light is visible in most experiments. The process responsible for $u_2(t)$ lasts only several µs and emits light of comparable intensity as the contracted plasmoid (see Figures 2, 3, and 7). To explain the origin of this second light, a physical (or chemical) reaction of the plasmoid components H, H_2, O, O_2, OH, H_2O can be assumed (in reference [15], the authors talk about unusual power-consuming compounds of oxygen and hydrogen present in the plasmoid). At present, however, it is still unclear what kind of physical (or chemical) reaction it should be. All that can be said is that, most probably, this reaction usually starts after the plasmoid is contracted sufficiently to a small volume and thus a very high pressure and temperature in the plasmoid is achieved. As can be seen in Figures 4 - 7, parameters d_{12}, δ_2, and u_{M2} grow almost linearly with the bubble size R_{M1} (parameter Δ also grows with R_{M1}, but steeper than linearly, see Figure 9 in [24]). Thus, the amount of substances entering into the chemical reaction will be proportional to the bubble size R_{M1}. However, nothing else can be deduced from the available experimental data at the present time. And no other quantitative data are available in the literature [9, 12, 13, 26].

After a careful observation of the shapes and widths of the light pulses $u_2(t)$ and after closer examination of the data given in Figure 7, we came to a conclusion that under certain circumstances, such as those occurring in laser-generated bubbles and in bubbles that are oscillating in acoustic resonators, the emission of light caused by the second process can be significantly increased compared to the emission caused by the first process. In that case, the value of u_{M2} may be much higher than the value of u_{M1}. If this assumption proves to be correct, then the light pulses observed in works [9, 12, 13, 26] are identical with the light pulses $u_2(t)$ observed in the present study.

Finally, it may be useful to compare different types of oscillating bubbles from the point of view of light emission. As mentioned in the Introduction, beside the spark-generated bubbles studied here, other types of bubbles were also intensively used to investigate light emission. Most extensive data on light pulses were obtained when studying laser-generated bubbles [8–10, 12, 13], and in the case of bubbles oscillating in acoustic resonators [22]. When comparing the experimental data on light emission from spark-generated bubbles with data measured with other types of bubbles, certain similarities and certain differences can be observed. The similarities can be seen, for example, in the values of the maximum surface temperatures of the emitting plasma. For different types of bubbles, these temperatures range from 4300 K to 8700 K [10, 18, 27, 28] (only bubbles oscillating in water under ordinary laboratory conditions are compared here). Authors of works [9, 12, 13] also mention the great scatter of the optical pulse maximum values, of the pulse widths, and of the pulse shapes. In the case of laser-generated bubbles [9, 12, 13], the multiple peaks in light flashes were also observed. And Moran and Sweider [26], who were studying bubbles in an acoustic resonator, also reported the occurrence of the first light pulse followed by a small second pulse, which they called "afterpulse". Finally, to close the discussion of the similarities, let us mention that even in the article of Baghdassarian et al. [8], the light emission during the whole first bubble oscillation T_{o1} can be seen in the published Figure 1.

However, there are also differences between the light flashes emitted from spark-generated bubbles and other types of bubbles. These differences can be seen, for example, in the shape of the light pulses and in the variation of the light pulse widths Δ with the bubble size R_{M1}. The shapes of the light pulses observed in the case of laser-generated bubbles and bubbles oscillating in acoustic resonators [8–10, 12, 26] are "Gaussian" and pulse widths increase almost linearly with the bubble size R_{M1} [8–10]. Unlike these observations, the shape of the light pulses $u_1(t)$ observed in our experiments is not "Gaussian" (see, e.g. Figures 1, 2, and 3) and pulse widths increase with the bubble size as $\sim R_{M1}^{3,3}$ [24]. In some experiments, the number of observed pulses was also greater than two. For example, Ohl [9] observed up to three local maxima before the main maximum and denoted these local maxima as precursors. As an explanation for these local maxima, he suggested that "the precursors originate from different hot spots; either a strongly

inhomogeneous bubble interior, or a splitting of the bubble into parts". Sukovich et al. [12] also observed that "many events were shown to have multiple peaks in the emission curve for a single event". And as an explanation of this, they said that "this likely suggests nonuniformities in either pressure or bubble distribution in the collapse region or that the conditions requisite for emissions are probabilistic in nature and so may occur at any point in space or time in the region so long as conditions are above some threshold value". Finally, Supponen et al. [13] reported that "the number of peaks in the photodetector signals varies between one and four, suggesting multiple events yielding light emission". The last-mentioned authors did not suggest any closer explanation for the origin of the events. Unfortunately, due to the lack of suitable experimental data, the causes of the differences between the spark-generated and laser-generated bubbles cannot be explained in greater detail at present.

5. Conclusion

In this work, the second light flashes emitted from the spark-generated bubbles in the final stages of the first bubble contraction and early stages of the following expansion were studied in detail. To obtain the necessary time information, optical waves $u(t)$ and acoustic waves $p(t)$ had to be simultaneously recorded. The large size of the generated bubbles also proved advantageous. To explain the existence of the observed two light flashes, two independent processes taking place in bubbles are assumed. The first process is responsible for the light emission during the whole first bubble oscillation, and it is believed that the nature of this process is similar to the process running in plasmoids. The second process, which is responsible for the second light flashes, is assumed to be a physical (or chemical) reaction of the plasmoid components. Experimental investigation of these processes taking place in bubbles under very high pressures and temperatures in a very limited space and lasting an extremely short time will require the development of new experimental techniques. Also, the very low reproducibility of spark-generated bubbles must be overcome. And the new technique should avoid averaging, unfortunately so common in studies of light emission from bubbles.

Acknowledgements

This work was partly supported by the Ministry of Education of the Czech Republic as a research project MSM 245 100 304. The experimental part of this work was carried out during the author's stay at the Underwater Acoustics Laboratory of the Italian Acoustics Institute, CNR, Rome, Italy. The author wishes to thank Dr. Silvano Buogo of the CNR-INSEAN Marine Technology Research Institute, Rome, Italy, for his very valuable help in preparing the experiments.

References

[1] G. L. Chahine, A. Gnanaskandan, A. Mansouri, et al. Interaction of a cavitation bubble with a polymeric coating–scaling fluid and material dynamics. *International Journal of Multiphase Flow* **112**:155 – 169, 2019. DOI:10.1016/j.ijmultiphaseflow.2018.12.014.

[2] P. A. Dayton, J. S. Allen, K. W. Ferrara. The magnitude of radiation force on ultrasound contrast agents. *The Journal of the Acoustical Society of America* **112**(5):2183–2192, 2002. DOI:10.1121/1.1509428.

[3] V. Sboros. Response of contrast agents to ultrasound. *Advanced Drug Delivery Reviews* **60**:1117–1136, 2008. DOI:10.1016/j.addr.2008.03.011.

[4] E. P. Stride, C. C. Coussios. Cavitation and contrast: The use of bubbles in ultrasound imaging and therapy. *Proceedings of the Institution of Mechanical Engineers, Part H: Journal of Engineering in Medicine* **224**(2):171–191, 2010. DOI:10.1243/09544119JEIM622.

[5] D. Thomas, M. Butler, N. Pelekasis, et al. The acoustic signature of decaying resonant phospholipid microbubbles. *Physics in Medicine and Biology* **58**:589–599, 2013. DOI:10.1088/0031-9155/58/3/589.

[6] T. Segers, N. de Jong, M. Versluis. Uniform scattering and attenuation of acoustically sorted ultrasound contrast agents: Modeling and experiments. *The Journal of the Acoustical Society of America* **140**:2506–2517, 2016. DOI:10.1121/1.4964270.

[7] B. Ward, D. Emmony. Interferometric studies of the pressures developed in a liquid during infrared-laser-induced cavitation-bubble oscillation. *Infrared Physics* **32**:489 – 515, 1991. DOI:10.1016/0020-0891(91)90138-6.

[8] O. Baghdassarian, B. Tabbert, G. A. Williams. Luminescence characteristics of laser-induced bubbles in water. *Physical Review Letters* **83**:2437–2440, 1999. DOI:10.1103/PhysRevLett.83.2437.

[9] C.-D. Ohl. Probing luminescence from nonspherical bubble collapse. *Physics of Fluids* **14**:2700–2708, 2002. DOI:10.1063/1.1489682.

[10] E. Brujan, D. Hecht, F. Lee, G. Williams. Properties of luminescence from laser-created bubbles in pressurized water. *Physical Review E, Statistical, Nonlinear, and Soft Matter Physics* **72**:066310, 2005. DOI:10.1103/PhysRevE.72.066310.

[11] C. Frez, G. Diebold. Laser generation of gas bubbles: Photoacoustic and photothermal effects recorded in transient grating experiments. *The Journal of Chemical Physics* **129**:184506, 2008. DOI:10.1063/1.3003068.

[12] J. R. Sukovich, A. Sampathkumar, P. A. Anderson, et al. Temporally and spatially resolved imaging of laser-nucleated bubble cloud sonoluminescence. *Physical Review E, Statistical, Nonlinear, and Soft Matter Physics* **85**:056605, 2012. DOI:10.1103/PhysRevE.85.056605.

[13] O. Supponen, D. Obreschkow, P. Kobel, M. Farhat. Luminescence from cavitation bubbles deformed in uniform pressure gradients. *Physical Review E, Statistical, Nonlinear, and Soft Matter Physics* **96**:033114, 2017. DOI:10.1103/PhysRevE.96.033114.

[14] Y. Sun, I. V. Timoshkin, M. J. Given, et al. Acoustic impulses generated by air-bubble stimulated underwater spark discharges. *IEEE Transactions on Dielectrics and Electrical Insulation* **25**(5):1915–1923, 2018. DOI:10.1109/TDEI.2018.007293.

[15] P. Golubnichy, Y. Krutov, E. Nikitin, D. Reshetnyak. Conditions accompanying formation of long-living luminous objects from dissipating plasma of electric discharge in water. *Voprosy Atomnoy Nauki i Tekhniki* pp. 143–146, 2008.

[16] Y. Huang, H. Yan, B. Wang, et al. The electro-acoustic transition process of pulsed corona discharge in conductive water. *Journal of Physics D: Applied Physics* **47**:255204, 2014. DOI:10.1088/0022-3727/47/25/255204.

[17] Y. Huang, L. Zhang, J. Chen, et al. Experimental observation of the luminescence flash at the collapse phase of a bubble produced by pulsed discharge in water. *Applied Physics Letters* **107**:4104, 2015. DOI:10.1063/1.4935206.

[18] L. Zhang, X. Zhu, H. Yan, et al. Luminescence flash and temperature determination of the bubble generated by underwater pulsed discharge. *Applied Physics Letters* **110**:034101, 2017. DOI:10.1063/1.4974452.

[19] A. Hajizadeh Aghdam, B. Khoo, V. Farhangmehr, M. T. Shervani-Tabar. Experimental study on the dynamics of an oscillating bubble in a vertical rigid tube. *Experimental Thermal and Fluid Science* **60**:299–307, 2015. DOI:10.1016/j.expthermflusci.2014.09.017.

[20] I. Ko, H.-Y. Kwak. Measurement of pulse width from a bubble cloud under multibubble sonoluminescence conditions. *Journal of The Physical Society of Japan* **79**:124401, 2010. DOI:10.1143/JPSJ.79.124401.

[21] T. G. Leighton, M. Farhat, J. E. Field, F. Avellan. Cavitation luminescence from flow over a hydrofoil in a cavitation tunnel. *Journal of Fluid Mechanics* **480**:43–60, 2003. DOI:10.1017/S0022112003003732.

[22] V. Borisenok. Sonoluminescence: Experiments and models (Review). *Acoustical Physics* **61**:308–332, 2015. DOI:10.1134/S1063771015030057.

[23] S. Buogo, K. Vokurka. Intensity of oscillation of spark-generated bubbles. *Journal of Sound and Vibration* **329**:4266–4278, 2010. DOI:10.1016/j.jsv.2010.04.030.

[24] K. Vokurka, S. Buogo. Experimental study of light emitted by spark-generated bubbles in water. *The European Physical Journal Applied Physics* **81**:11101, 2018. DOI:10.1051/epjap/2017170332.

[25] K. Vokurka. The time difference in emission of light and pressure pulses from oscillating bubbles. *Acta Polytechnica* **58**:323, 2018. DOI:10.14311/AP.2018.58.0323.

[26] M. J. Moran, D. Sweider. Measurements of sonoluminescence temporal pulse shape. *Physical Review Letters* **80**:4987–4990, 1998. DOI:10.1103/PhysRevLett.80.4987.

[27] K. Vokurka. Experimental determination of temperatures in spark-generated bubbles oscillating in water. *Acta Polytechnica* **57**:149–158, 2017. DOI:10.14311/AP.2017.57.0149.

[28] K. Vokurka, J. Plocek. Experimental study of the thermal behavior of spark generated bubbles in water. *Experimental Thermal and Fluid Science* **51**:84–93, 2013. DOI:10.1016/j.expthermflusci.2013.07.004.

[29] A. Egorov, S. Stepanov. Properties of short-lived ball lightning produced in the laboratory. *Technical Physics* **53**:688–692, 2008. DOI:10.1134/S1063784208060029.

[30] S. Shevkunov. Cluster mechanism of the energy accumulation in a ball electric discharge. *Doklady Physics* **46**:467–472, 2001. DOI:10.1134/1.1390398.

[31] S. Shevkunov. Scattering of centimeter radiowaves in a gas ionized by radioactive radiation: Cluster plasma formation. *Journal of Experimental and Theoretical Physics* **92**:420–440, 2001. DOI:10.1134/1.1364740.